IOP Conf. Series: Materials Science and Engineering **233** (2017) 012007 doi:10.1088/1757-899X/233/1/012007

Cavitation in centrifugal pump with rotating walls of axial inlet device

O Moloshnyi[1], M Sotnyk[1]

[1]Applied Hydro- and Aeromechanics department, Faculty of Technical Systems and Energy Efficient Technologies, Sumy State University, Sumy 40007, Ukraine

E-mail: o.moloshnij@pgm.sumdu.edu.ua

Abstract. The article deals with the analysis of cavitation processes in the flowing part of the double entry centrifugal pump. The analysis is conducted using numerical modeling of the centrifugal pump operating process in the software environment ANSYS CFX. Two models of the axial inlet device is researched. It is shaped by a cylindrical section and diffuser section in front of the impeller, which includes fairing. The walls of the axial inlet device rotate with the same speed as the pump rotor. The numerical experiment is conducted under the condition of the flow rate change and absolute pressure at the inlet. The analysis shows that the pump has the average statistical cavitation performance. The occurrence of the cavitation in the axial inlet device is after narrowing the cross-section of flow channel and at the beginning of the diffuser section. Additional sudden expansion at the outlet of the axial inlet diffuser section does not affect the cavitation characteristics of the impeller, however, improves cavitation characteristics of the axial inlet device. For considered geometric parameters of the axial inlet device the cavitation in the impeller begins earlier than in the axial inlet device. That is, the considered design of the axial inlet device will not be subjected to destruction at the ensuring operation without cavitation in the impeller.

1. Introduction

Cavitation is a negative phenomenon that can occur in a pump. It leads to the destruction of the material, the occurrence of vibration and noise, reduction of the head and the efficiency of the pump. Scientists have devoted much attention to researching the cavitation and ways to reduce the probability of its occurrence in the pumps. One of the methods to fight against the occurrence of the cavitation in a centrifugal pump impeller is an additional inducer in front of it. Guo et.al [1] analyzed the influence of inducer with different designs on the cavitation characteristics of the centrifugal pump. The authors determined by the numerical simulation and confirmed experimentally that long inducer has better anti-cavitation characteristics than a short one. Although, the use of an inducer is considered an effective way to fight against the cavitation, however, there are many other ways. Xie et.al [2] investigated the influence of slots with different configurations in the impeller blades near the leading edge on the distribution of vapour volume fraction in the impeller and cavitation characteristics of the pump. The authors found that the slots with a large diameter and a smaller angle to the tangent of the impeller eye improve cavitation characteristics and does not affect the efficiency of the pump. Si et.al [3] found improved cavitation characteristics of the centrifugal pump with an additional jetting pipe in the pump inlet nozzle. However, cavitation characteristics get worse with increase of the flow rate. Zhuang et.al [4] got worse pump cavitation characteristics of the double entry pump with the radial

blades of the impeller than the profiled. Tan et.al [5] found deterioration of the cavitation characteristics in the case of the prewhirl regulation by inlet guide vanes in front of the impeller. Hergt et.al [6] described the best known ways to improve the cavitation performance. The authors noted the impact of a diffuser on the shortening the recirculation zone length and the reducing the risk of cavitation. In addition, Gülich [7] noted the efficiency of using the diaphragm to reduce the cavitation. Kozubkováa et.al [8] researched the cavitation in the diffuser using different models of the cavitation and found a little difference in the results.

2. Models and Boundary Conditions

2.1. Pump geometry mode

The main pump parameters are as follows: nominal flow rate Q_{nom} = 25 m^3/h, head H=12 m, rotational speed n = 1450 r.p.m, specific speed n_q = 13 rpm, impeller eye diameter D_0 = 75 mm impeller outer diameter D_2 = 202 mm, the number of impeller blades z = 7.

The pump axial inlet device is a hollow shaft, which is also simultaneously the pump shaft. It is shaped by cylindrical and diffuser area in front of the impeller, which includes fairing (Figure 1). In addition, an axial cylindrical section of the casing is situated before the axial inlet device.

The numerical simulation of the fluid flow is conducted for 2 axial inlet device models (Figure 1). The design of Model 2 additionally comprises a sudden expansion at the exit of diffuser section. The diameter of the cylindrical section d and the inlet D are 45 mm and 65 mm respectively. The length of rotational wall of the axial inlet device is L = 227 mm and the stationary section of the casing is l = 40 mm. The length of the fairing (l_f) and the diffuser section of the axial inlet device (l_{dif}) are 37 mm and 50 mm respectively, an external (D_{out}) diameter of the outlet of the diffuser section in the model №1 and №2 are 75 mm and 71 mm respectively. The internal (d_{out}) diameter of the outlet of the diffuser section is 40 mm. Axial dimensions of the pump housing limit the axial inlet device dimensions.

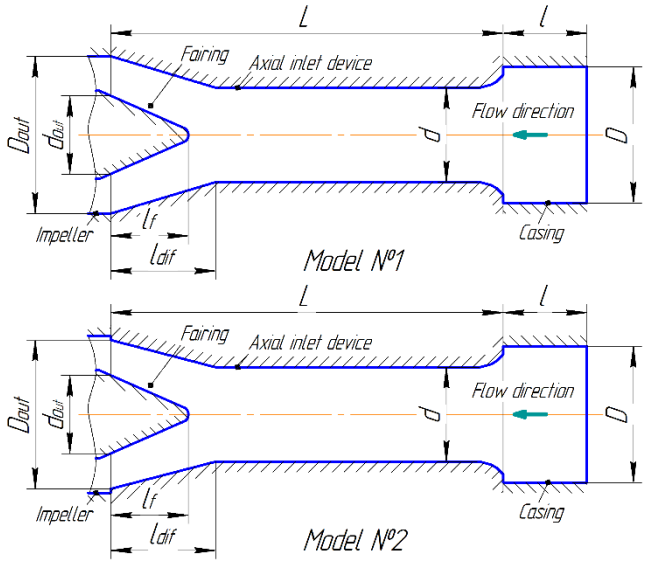

Figure 1. Scheme of the axial inlet device.

2.2. Mesh generation and boundary conditions

A solid model of a fluid computational domain of the double entry centrifugal pump includes the inlet pipe, the outlet pipe, the axial inlet device, the impeller and the annular casing with guide vanes (Figure 3). A geometry of the flowing part was simplified by assumptions about the absence of a sinus pump. Also, symmetry flow relative to the impeller of the double entry centrifugal pump was considered. This reduces complexity and increases the speed of calculation.

An unstructured mesh is generated using software ICEM-CFD (Figure 2). Elements size is selected via mesh independence research. Layers of prismatic elements were created near solid walls in the boundary layer (Figure 3(b)). In addition, elements of the mesh near the leading edge and the trailing edge are smaller. The total number of elements of the pump flowing part is 5 million. The inlet device, the impeller and the annular casing contain 0.97 mln, 2.4 mln and 1.65 mln of elements respectively.

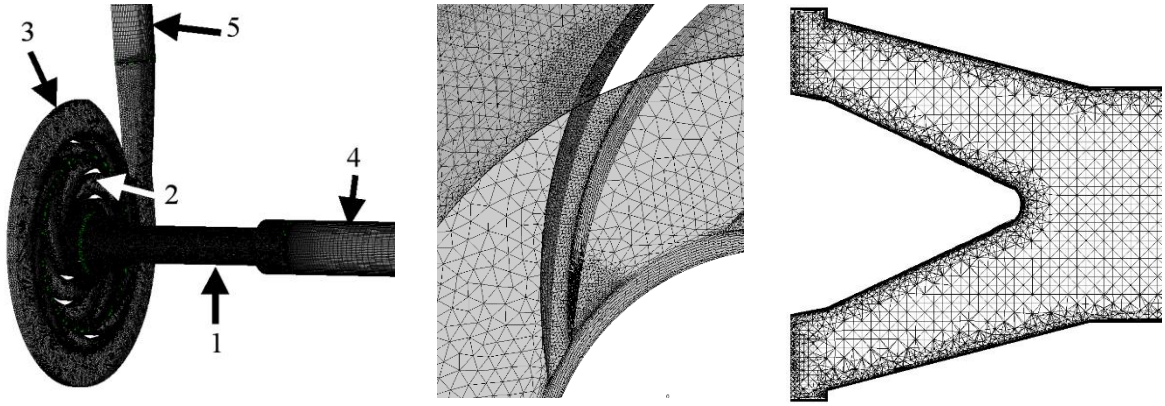

(a) (b) (c)

Figure 2. Calculation mesh: (a) computational domains: 1 – axial inlet device, 2 – impeller, 3 – annular casing, 4 – inlet pipe, 5 – outlet pipe; (b) leading edge; (c) diffuser section of the inlet device.

The numerical simulation of fluid flow in the flowing part of the pump was conducted using the software ANSYS CFX. To get cavitation characteristics was used the Rayleigh-Plesset equation, the standard k-ε turbulence model and Reynolds equation [9]. Boundary conditions was set as: the total pressure at the pump inlet and the mass flow rate at the pump outlet. The numerical calculation was carried out at the flow rate (0.7; 1.0; 1.2) Q_{nom}. Working fluid was water and water-vapor at temperature 25˚C. The saturated steam pressure was set as 3167 Pa. The roughness of the axial inlet device surfaces was adopted 6.3 microns.

3. Results analysis

3.1. HPSH analysis

The results of the numerical simulation define the cavitation performance of the pump at the flow rates (0.7; 1.0; 1.2) Q_{nom} (Figure 3). The cavitation performance of Model 1 and Model 2 are qualitatively and quantitatively similar despite the introduction of the sudden expansion at the outlet of the axial inlet device. Minor differences in the magnitude of the head drop between the models observed. Also, there is a slight head drop and rise before its rapid decline. The head drop in Model 2 for the flow rate 1.2 Q_{nom} at NPSH more than 3 m hardly occurs. The above discussed differences do not affect $NPSH_3$, defined head drop by 3%. It is 0.15 m, 0.31 m and 0.45 m respectively for the flow rate (0.7; 1.0; 1.2) Q_{nom} for both models. $NPSH_A$ [7] is respectively 0.75 m, 0.91 m and 1.05 m.

An important criterion for cavitation in a pump is the suction specific speed n_{ss} [7]. It is defined as:

$$n_{ss} = n\frac{\sqrt{Q_{nom}/f_q}}{NPSH_3^{0.75}}$$

where, n is rotation speed; f_q is impeller eyes per impeller.

The values of the suction specific speed at the flow rate Q_{nom} for both models are 206. Standard impellers for axial inlet or between-bearing pumps have a value in the range of 160 - 220 [7]. That is, the indicator of the studied pump is above the average.

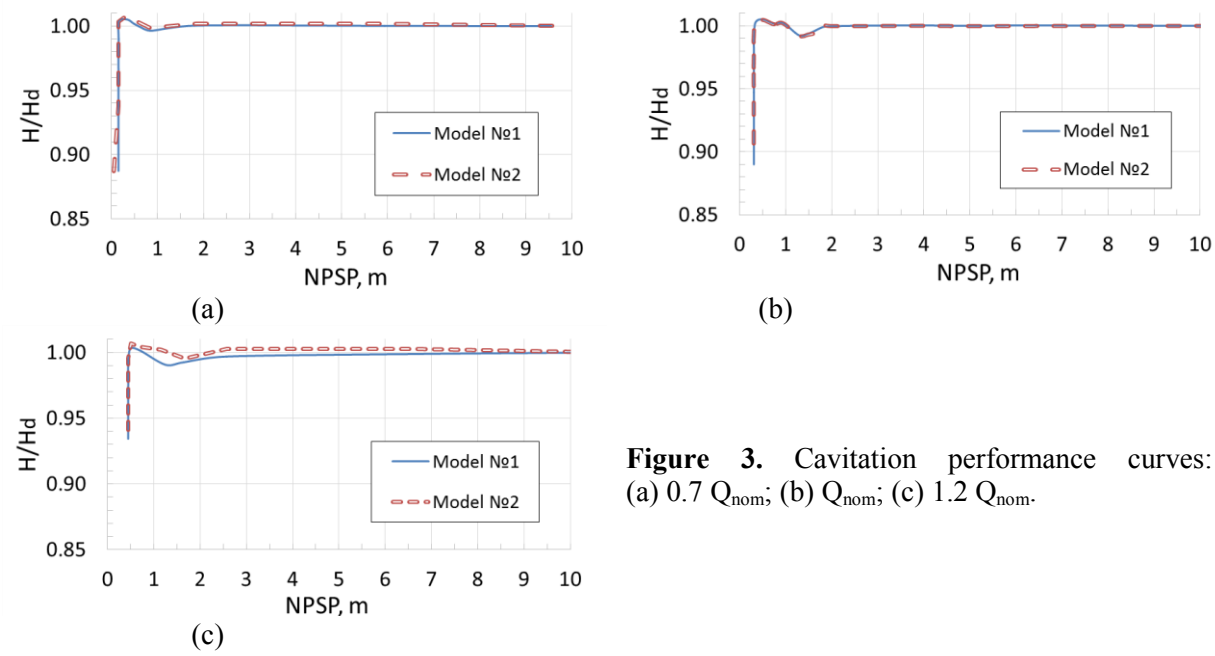

Figure 3. Cavitation performance curves: (a) 0.7 Q_{nom}; (b) Q_{nom}; (c) 1.2 Q_{nom}.

3.2. Cavitation structure and vapour volume fraction distribution

The occurrence of the cavitation in the impeller at the flow rate Q_{nom} is observed at the NPSP = 2 m (Figure 4(a)). It appears on the suction surface of the blades and almost does not effect the discharge characteristics of the pump. The cavitation zones are increased by reducing the NPSH (Figure 4(b)). At the NPSH3 there is a significant cavitation near the suction surface of the blades, which occupies a significant part of the passage between the blades (Figure 4 (c)). Distribution cavitation zones in the impeller for both models are almost identical.

The size of cavitation zones while reducing cavitation pressure of 3% is different for different flow rate. The cavitation zones and vapour fraction decrease under the condition of increasing the flow rate from 0.7 Q_{nom} to 1.2 Q_{nom} (Figure 5). The same pattern appears with other values of the head drop. Also, there is a slight increase of the cavitation zones at the constant value of the NPSH and increasing the flow rate (Figure 6). This is the result of the changing the approach flow angle, which depends on the value of the velocity and direction of the flow at the impeller inlet. It should be noted that the value of the circumferential component of the absolute velocity is also affected by the rotation of the walls.

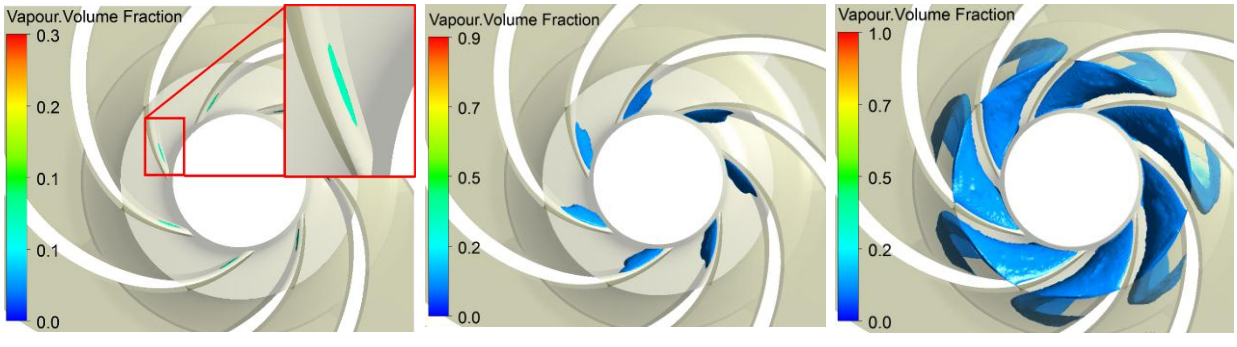

Figure 4. Cavitation structure in the impeller at Q_{nom}: (a) NPSP = 2 m; (b) NPSP = 1 m; (c) $NPSP_3$ = 0.31 m.

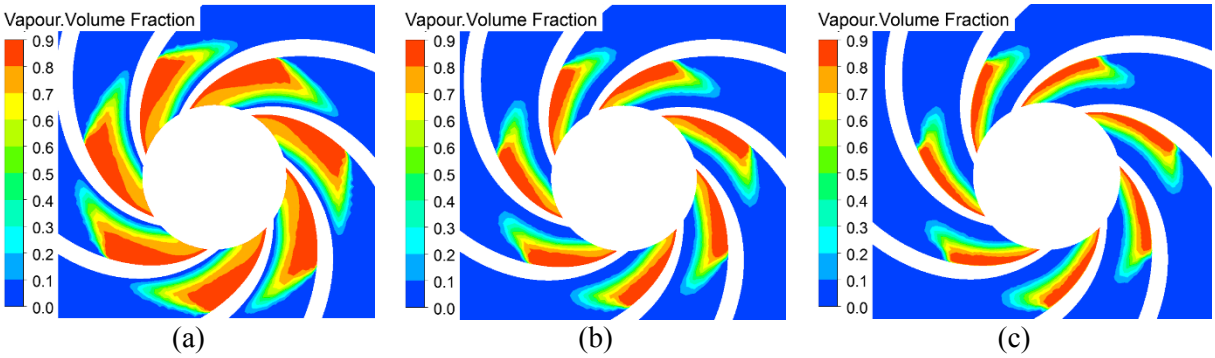

Figure 5. Vapour volume fraction distribution in the impeller: (a) $NPSP_3$ = 0.15 m, 0.7 Q_{nom}; (b) $NPSP_3$ = 0.31 m, Q_{nom}; (c) $NPSP_3$ = 0.45 m, 1.2 Q_{nom}.

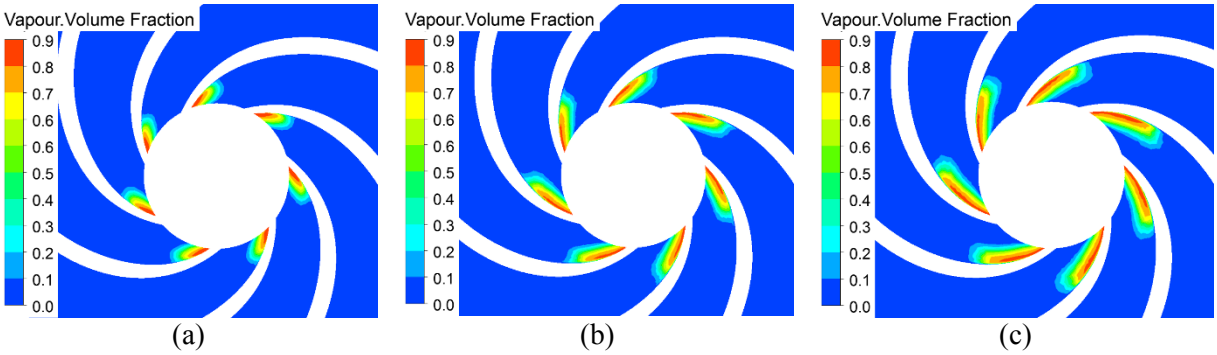

Figure 6. Vapour volume fraction distribution in the impeller at NPSP = 0.5 m: (a) 0.7 Q_{nom}; (b) Q_{nom}; (c) 1.2 Q_{nom}.

The cavitation occurs in the axial inlet device at the NPSP is 0.17 m, 0.35 m and 0.5 m respectively at the flow rate (0.7; 1.0; 1.2) Q_{nom} in both models. There are two cavitation zones (Figure 7). The first zone is after narrowing the cross-section of flow channel. The second zone is at the beginning of diffuser section of the axial inlet device. It should be noted that cavitation in the impeller starts earlier than in the axial inlet device. $NPSH_A$ for the impeller is higher than NPSP where there are first signs of cavitation in the axial inlet device. That is, the first destruction must be occur in the impeller.

The occurrence of the cavitation zones for different flow rate and the models of the axial inlet device are the same but have different dimensions (Figure 8). The cavitation zones in Model 1 are relatively higher than in Model 2, especially it is manifested at the flow rate 0.7 Q_{nom} and 1.2 Q_{nom}. To some extent this is due to the decrease of the angle diffuser disclosure. The difference value of the zone volume is greater under the condition of the greater flow rate. There are major cavitation zones and vapor particles in them at the flow rate 1.2 Q_{nom} in Model 1. The first zone is stretched along the walls of the cylindrical section of the axial inlet device. The second zone occupies a significant part of the diffuser section. In addition, the cavitation appears in the third zone, located near the fairing at the outlet of the diffuser section.

Figure 7. Cavitation structure in the axial inlet device at Q_{nom}: (a) NPSP = 0.35 m; (b) $NPSP_{3\%}$ = 0.31 m;

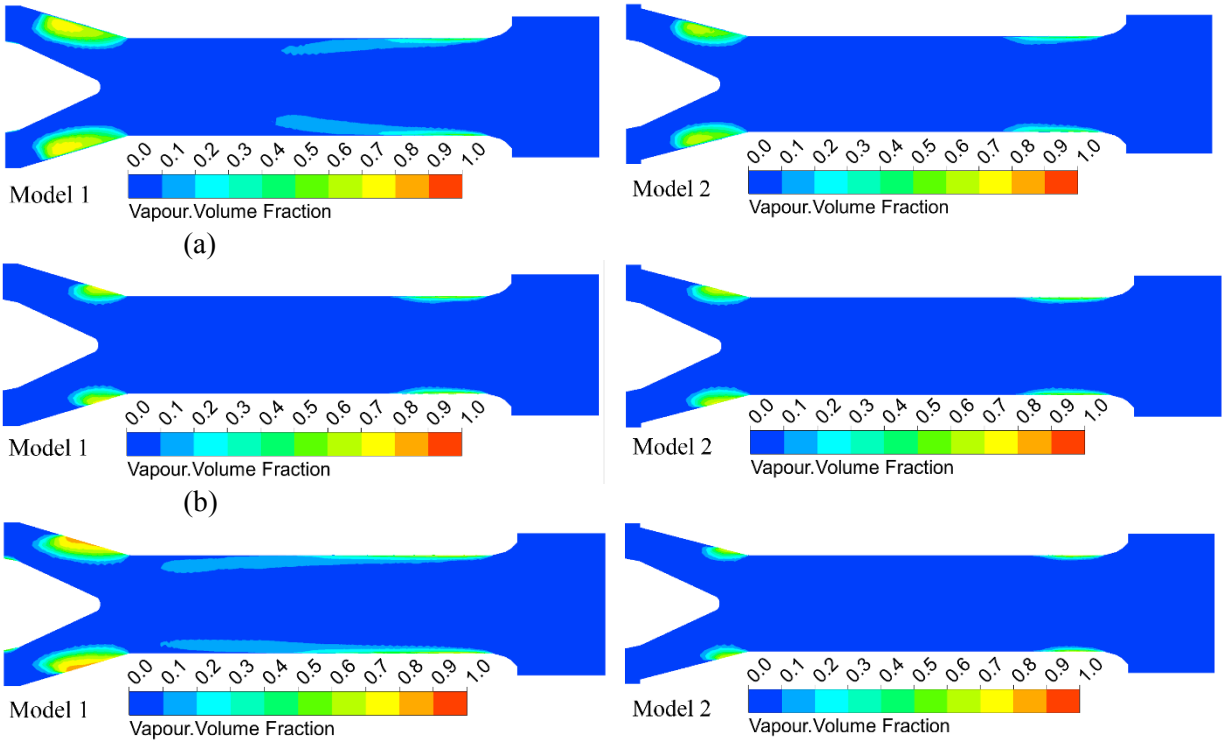

Figure 8. Vapour volume fraction distribution in the axial inlet device: (a) $NPSP_3$ = 0.15 m, 0.7 Q_{nom}; (b) $NPSP_3$ = 0.31 m, Q_{nom}; (c) $NPSP_3$ = 0.45 m, 1.2 Q_{nom}.

3.3. Pressure distribution

The absolute pressure distribution in the impeller for a different NPSP is similar (Figure 9). It should be noted that at the NPSP = 2 m the minimum absolute pressure in the impeller is much more than the saturation pressure, however, the cavitation at the suction surface of the blades already happens.

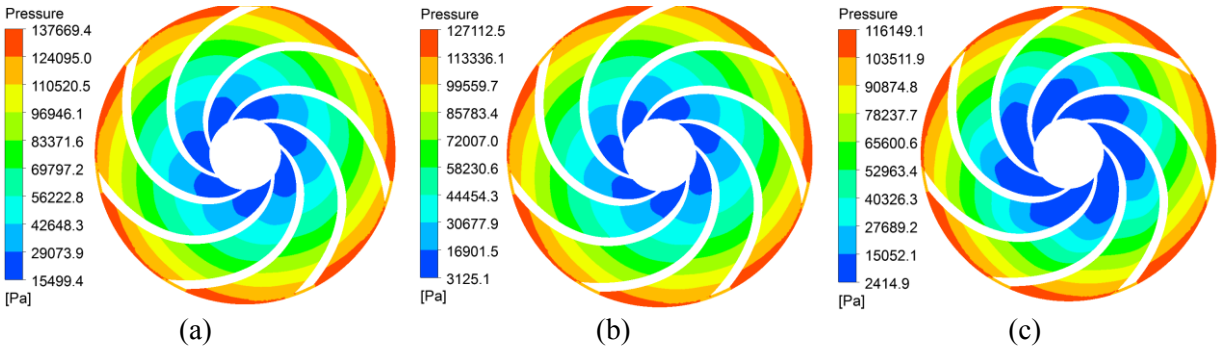

Figure 9. Absolute pressure distribution in the impeller at Q_{nom}: (a) NPSP = 2 m; (b) NPSP = 1 m; (c) $NPSP_3$ = 0.31 m.

The absolute pressure distribution in the axial inlet device demonstrates the zones of the reduced pressure (Figure 10, 11). The first zone is after narrowing cross-section, and the second zone is at the beginning of the diffuser section. The increasing of the flow velocity and the whirls occur in these zones. With the passage of fluid zones there is a significant decrease in pressure, which causes the cavitation. The absolute pressure distribution for both models is similar with the corresponding values of $NPSP_3$ for the considered flow rates (Figure 11). However, the minimum value of the absolute

pressure in Model 2 is bigger than in Model 1. This explains the reduction of the cavitation zones in Model 2. In the larger flow rate the pressure difference is also greater.

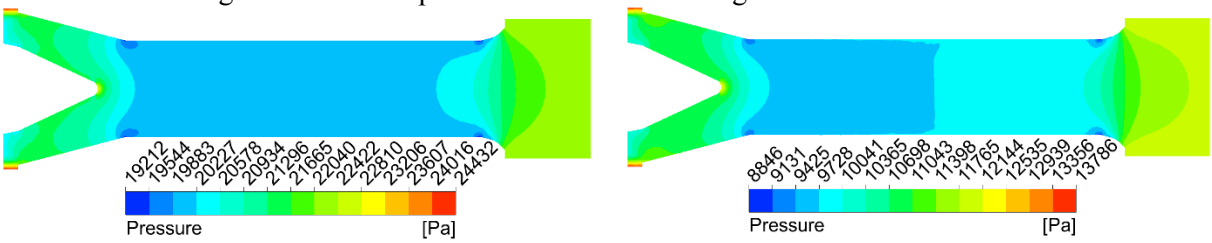

Figure 10. Absolute pressure distribution in Model 1 of the axial inlet device at Q_{nom}: (a) NPSP = 2 m; (b) NPSP = 1 m.

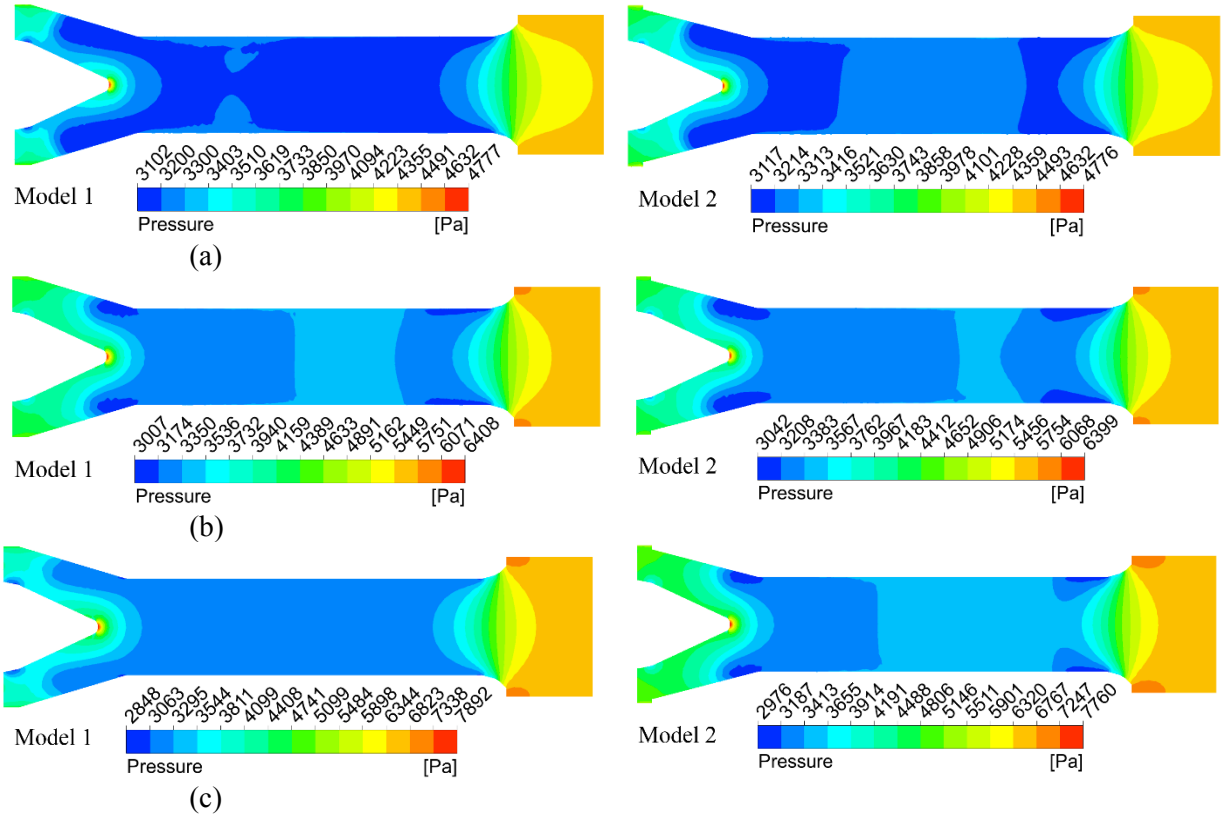

Figure 11. Absolute pressure distribution in the axial inlet device: (a) $NPSP_3$ = 0.15 m, 0.7 Q_{nom}; (b) $NPSP_3$ = 0.31 m, Q_{nom}; (c) $NPSP_3$ = 0.45 m, 1.2 Q_{nom}.

To eliminate the first zone of the absolute pressure reduction it is necessary to eliminate the change of the diameters at the inlet of the axial inlet device. That means, it is necessary to reduce the diameter of the pump inlet to the size of the cylindrical section diameter of the axial inlet device. To eliminate the second zone is necessary to eliminate abrupt change from the cylindrical to the diffuser section.

4. Conclusion

Analysis of the numerical simulation results of the operating process in the double entry centrifugal pump provided changes of the geometric parameters of the diffuser section of the axial inlet device with rotating walls at the flow rate (0.7; 1.0; 1.2) Q_{nom} enables the following conclusions:

1) Both models $NPSH_3$ is 0.15 m, 0.31 m and 0.45 m respectively for the flow rate (0.7; 1.0; 1.2) Q_{nom}. $NPSH_A$ is respectively 0.75 m, 0.91 m and 1.05 m. In this case, for exploitation of the pump without cavitation NPSH must be more than 2 m. The suction specific speed at Q_{nom} is 206 for both models.

2) When changing the flow rate the distribution of the cavitation zones in the impeller is similar, however the size of these zones is reduced with increasing the flow rate from 0.7 Q_{nom} to 1.2 Q_{nom}.

3) The cavitation in the impeller beginning earlier than in the axial inlet device. That is, the considered design of the axial inlet device will not be subjected to destruction at the ensuring operation without cavitation in the impeller.

4) Additional sudden expansion at the outlet of the axial inlet diffuser section does not affect the cavitation characteristics of the impeller, however, improves cavitation characteristics of the axial inlet device due to the decrease of the angle diffuser disclosure

5) To increase the cavitation characteristics of the axial inlet device it is necessary to reduce the pump inlet diameter to the size of the cylindrical section diameter and to eliminate abrupt change from the cylindrical to the diffuser section of the axial inlet device.

References

[1] Guo X, Zhu Z, Cui B and Li Y 2012 Analysis of cavitation performance of inducers, Centrifugal pumps (Dr. Dimitris Papantonis (Ed.), InTech)

[2] Xie S F, Wang1 Y, Liu Z C, Zhu Z T, Ning C and Zhao L F 2015 Optimization of centrifugal pump cavitation performance based on CFD. *International Symposium of Cavitation and Multiphase Flow (ISCM 2014) IOP Conf. Series: Materials Science and Engineering* **72** 032023

[3] Si Q, Yuan S, Yuan J, Bois G 2016 Investigation on the influence of jetting equipment on the characteristics of centrifugal pump *Advances in Mechanical Eng.* **8** (8) pp 1–11

[4] Zhuang B, Luo X, Zhu L, Wang X and Xu H 2011 Cavitation in a shaft-less double suction centrifugal miniature pump *International J. of Fluid Machinery and Systems* **4 (**1)

[5] Tan L, Zha L, Cao1 S L, Wang Y C and Gui S B 2015 Cavitation performance and flow characteristic in a centrifugal pump with inlet guide vanes *International Symposium of Cavitation and Multiphase Flow (ISCM 2014) IOP Conf. Series: Materials Sci. and Eng.* **72** 032028

[6] Hergt P, Nicklas A, Mollenkopf G and Brodersen S 1996 The suction performance of centrifugal pumps possibilities and limits of improvements *Proceedings of the international pump users symposium, Texas A&M University system* 13-26

[7] Gülich J F 2014 Centrifugal Pumps 3rd Edition (Springer Berlin, Heidelberg, New York)

[8] Kozubkováa M, Rautováb J, Bojkoc M 2012 Mathematical model of cavitation and modelling of fluid flow in cone *Procedia Engineering* **39** pp 9 - 18

[9] ANSYS CFX Reference Guide, Release 15.0. 2013. http://www.ansys.com